SiPM

Valentina Guglielmi, Alberto Gianvecchio, Fabio Coldani

June 18, 2019

Academic Year 2018/2019
Esperimentazioni di Fisica Nucleare e Subnucleare

Abstract

The main goal of this experiment is to understand the operating principle of a SiPM (Silicon photomultiplier). Firstly, characterizing quantities of SiPMs have been studied, such as Dark Counts, Crosstalk, Afterpulses and the response to light. Secondly, SiPMs have been used to characterize three different scintillators in terms of background noise, time response, light yield and energy resolution. In the end, radioactive sources as ^{90}Sr, ^{22}Na and ^{57}Co have been used to study the absorption of the emitted radiation in different materials and to acquire β and γ spectra.

Contents

1 A brief Introduction **3**

2 Experimental set Up **3**

3 Characterization **4**
3.1 Dark Counts[1] 4
3.2 First SiPM 5
3.3 Mini Spectrometer 6

4 LED emitter **7**
4.1 Conversion ADC to Voltage 7
4.2 Poisson distribution and Staircase 8
4.2.1 Peaks vs OverVoltage 8

5 Crystals **9**
5.1 Response Time 9
5.2 Background Noise 10
5.3 ^{22}Na Spectrum 11
5.4 ^{57}Co Spectrum 11
5.5 Light Yield 12
5.6 Energy Resolution 13
5.7 Barycenter of Absorption Crystals 14
5.8 Absorption 14
5.8.1 The case of Air 15
5.9 Cosmic Rays 16
5.10 β Spectroscopy 17

6 Conclusion and Comments **19**

1 A brief Introduction

The SiPM[1] is a silicon photomultiplier. It consists of a dense array of SPAD (Single photon avalanche diode) in parallel, each one with an integrated quenching resistor, as shown in figure (1). When an applied reverse bias voltage is sufficiently strong, higher than a certain breakdown voltage, photons can be absorbed by silicon and electron-hole pairs are generated. If the charged carrier (electron or hole) has a sufficient kinetic energy, secondary pairs are created. The formation of new pairs sets off an ionization avalanche that generates a net current flow, then quenched by the series resistor.

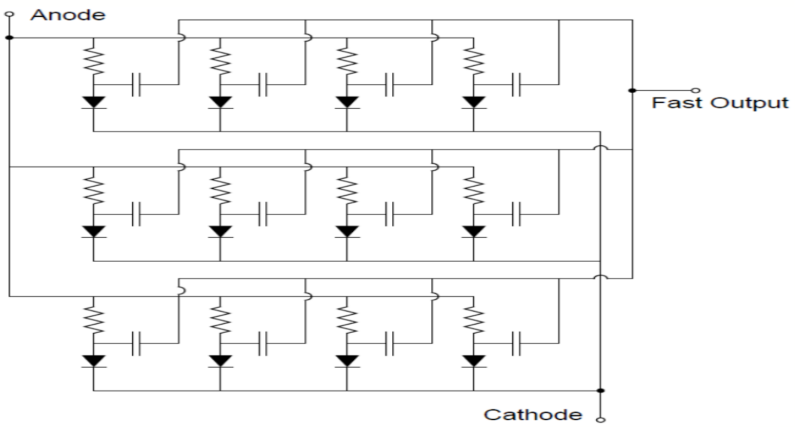

Figure 1: *A SiPM consists of an array of microcells with summed output.*

2 Experimental set Up

The set up of the experiment consists of more units:

- Three types of SiPMs: a mini spectrometer, a plastic scintillator and a general purpose one (sensor holder)

- PSAU[2]: This unit is a general purpose Power Supply and Amplification Unit, integrating up to two SiPMs. It features two channels with an independent Gain control up to 50 dB, and it provides the bias Voltage (up to 100V)

- DIGITIZER[2]: It converts the analogic signal coming from the SiPM in order to transmit data to a PC

- SOFTWARE CAEN

- LED Emitter[2]: unit capable of producing light signals at high and low frequency, with an optic fiber. The led pulse generation can be triggered by an

internal oscillator or by an external pulse

- Inorganic Scintillators: LYSO, BGO, CsI

- Optical Grease: Used in order to avoid discontinuity of refracting index between the SiPM and crystals

- Radioactive sources (^{22}Na, ^{57}Co, ^{60}Co ^{90}Sr)

3 Characterization

The first thing to do is to characterize the SiPM by studying its properties when it is not connected to light. The setup consists of a PSAU connected to a Digitizer and both to an Oscilloscope, even though the latter is not strictly necessary for the purpose of the characterization. Both the PSAU and the Digitizer are connected to the PC in order to transmit the data to a Software, developed by CAEN, which processes them.
The studies concern the characterization of Dark Counts, CrossTalks, the relation that exists between these quantities and the OverVoltage and how much the noise influences these physical measurements.

3.1 Dark Counts[1]

The main source of noise in an SiPM is the dark count rate (DCR), which is primarily due to thermal electrons generated in the active volume.
It is possible to characterize the rate of Dark Counts at different values of overvoltage ($V - V_{op}$)[1]. The software plots a staircase, which shows the dependence between the threshold (mV) and the number of events per unit time and area (Hz). An event is counted when an active cell is hit by one or more photons. Different measurements were taken for two distinct SiPMs. The first one is directly connected (figure(2)) to the PSAU, avoiding noises generated by pulses of environmental light and by wiring cables, the second one is integrated into a barrel covered by a black cloth. However, as shown figure(6), it is not possible to completely ignore the noise.

[1]The overvoltage is commonly defined for SiPM as $V_{bias} - V_{break}$. $V_{break}$is the bias point at which the electric field is sufficiently high ot create a geiger discharge. However, for the purpose of this experiment, Overvoltage has been defined as ($V - V_{op}$), where V_{op} is usually 10%-25% higher than the V_{break}

3.2 First SiPM

Figure 2: *The breakdown voltage is 54.96V*

The software acquires the number of photons hitting a pixels, which is expressed as a function of the number of charged ADC channel and consequently plots it as an histogram(figure 3). Each point of the staircase is obtained from the progressive integration of the bins of such histogram. Dark count is defined as the frequency corresponding to the first step of the staircase, while Crosstalk is defined as:

$$\frac{DCR_{1.5}}{DCR_{0}.5} \tag{1}$$

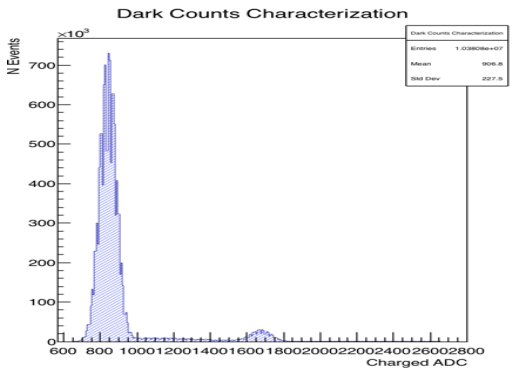

(a) Histogram, the first peak refers to one photon hitting a pixel

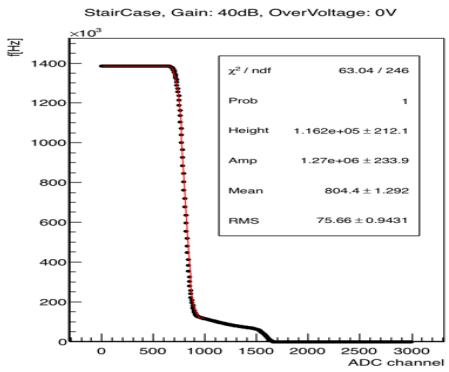

(b) Staircase, obtained from the integration of the histogram. The points are fitted with a sum of sigmoides (computed with error function centered in the point of inflection).

Figure 3: *Estimation of dark counts and overvoltage*

The relationship between Dark Counts versus overvoltage and Crosstalk versus overvoltage is expected to be linear(see figure(4)).

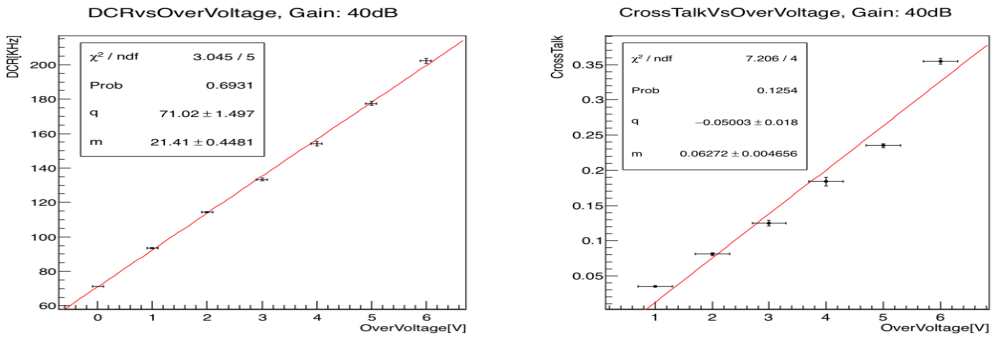

(a) The height of the fitting function added to its amplitude is the rate dark counts

(b) Crosstalk has been calculated as the height of the fitting function (frequency of the second step) over the rate of dark counts

Figure 4: *DC vs OverVoltage and Ct vs OverVoltage*

3.3 Mini Spectrometer

The procedure followed for the second SiPM is the same as the one used for the first. Although the Spectrometer(figure(5)) has been covered with a black cloth, it has not been possible to avoid noise effects due to the presence of light.

Figure 5: *The breakdown voltage is 54.96V*

Therefore, an estimation of crosstalk couldn't be found. As a matter of fact, in order to have a good fit of the staircase function (see figure(6)) a noise term (exponential or linear) has been added, precluding the estimation of the height of the second step.

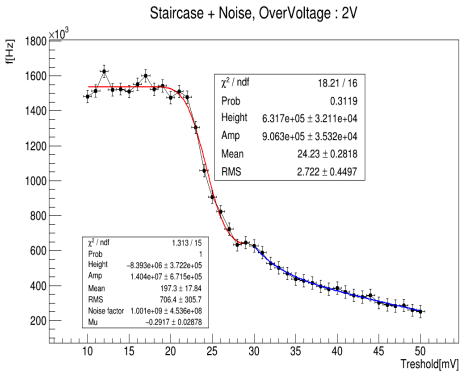

(a) erf(1) + erf(2) + exp

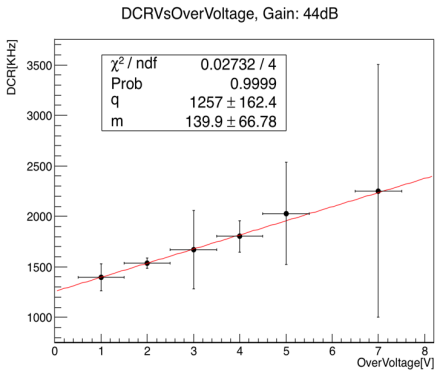

(b) Linear dependence

Figure 6: *Staircase and linear relationship*

4 LED emitter

4.1 Conversion ADC to Voltage

The first SiPM is connected to the LED emitter by an optical fiber. The Histogram acquired by the software is drawn in terms of counts versus charged ADC channels(figure(7)). The calculation of the the conversion factor between ADC and the Voltage is easily computed with an oscilloscope.
The ADC value of each peak is obtained as the mean (μ) of a Normal Distribution and the corresponding mV value is the amplitude of the wave shown on the oscilloscope.

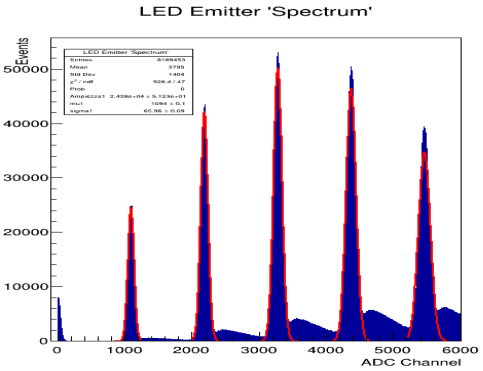

(a) Uncertainty on ADC is given by the fit error

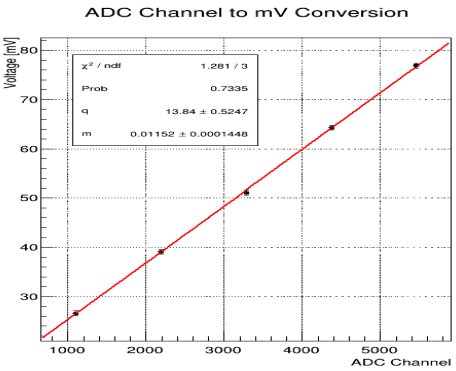

(b) The line does not pass from (0,0) so that the conversion value is also given by intercept

Figure 7: *Conversion ADC to mV*

$$\xi = (0.01152 \pm 0.00015)\frac{mV}{ADC} + (13.840 \pm 0.525)mV \tag{2}$$

4.2 Poisson distribution and Staircase

Following the same process that had been used in absence of light, and integrating the Histogram over different ranges, it has been possible to extract a staircase plot. Every peak is a photon or more hitting a cell; more precisely, the N-th peak refers to the emission of N photons(figure(8)).

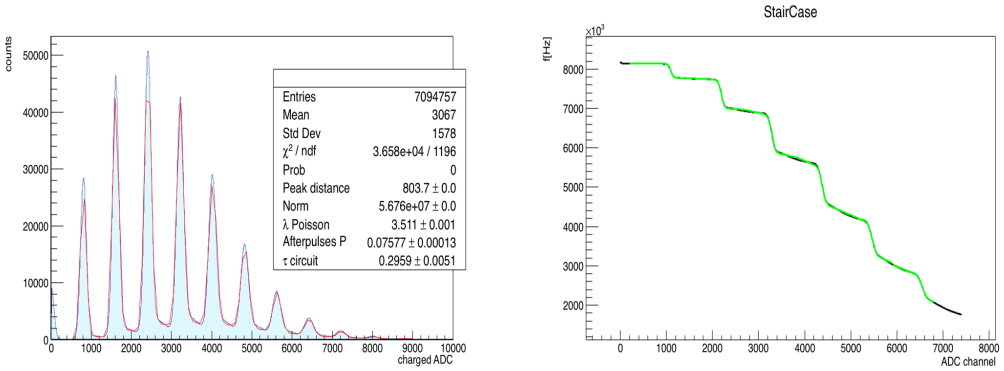

(a) Poisson distribution of peaks + afterpulses model

(b) Staircase fitted with a sum of sigmoides and linear noise

Figure 8: *Poisson distribution of the peaks*

4.2.1 Peaks vs OverVoltage

This section shows that the position of peaks grows as the Overvoltage is increased(figure 9). This effect is caused by a growth in the number of free charge carriers released during the avalanche process. The real position of each peak is taken as the centre of its normal distribution.

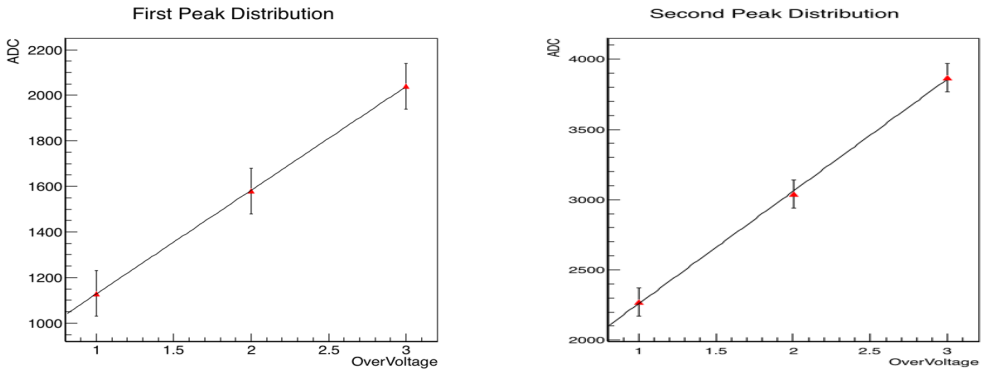

(a)

(b)

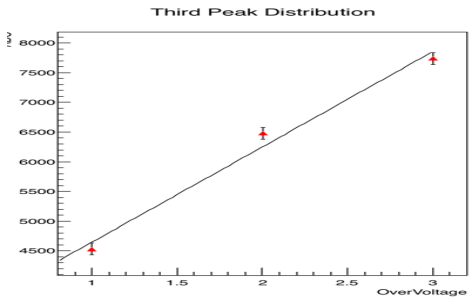

Figure 9: *From left to right: 1st peak, 2nd peak, 3rd peak*

5 Crystals

The focus of this section is to characterize different crystals in terms of their background noise, response time, light yield and energy resolution.
Crystals:

- LYSO (Lutetium-yttrium oxyorthosilicate)
- BGO $Bi_4Ge_3O_{12}$
- CsI

Each Crystal is inserted in the apposite space above the SiPM.

5.1 Response Time

The response and rise time have been estimated for each crystal. Several wave forms, produced by radioactive decays of ^{22}Na and ^{60}Co, have been acquired, averaged and fitted with a rising (as for a RC circuit) function and a decreasing one(figure (10)).

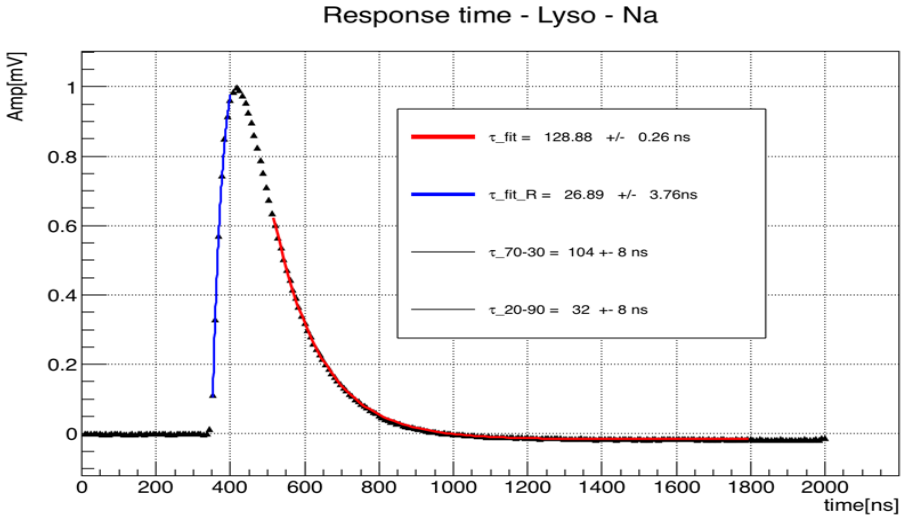

Figure 10: *LYSO: ^{22}Na*

The estimation of τ has been calculated both from the fit and from the difference between the time at 70% and at 30% along the decrease. Similarly, it has been subtracted the time at 20% from the time at 90% in order to study the rise.
These selections have been made under the assumption that the characteristic time of the circuit could be neglected, since in such short ranges the crystal alone is relevant for the evaluation of the response time.
This is not completely true for the LYSO scintillator, which has a shorter response time with respect to that of the circuit. The results are reported below:

Crystal	τ_{dec} **[ns]**	τ_{70-30} **[ns]**	τ_{rise} **[ns]**	τ_{20-90}**[ns]**
LYSO	128.82 ± 0.27	120.5 ± 11.3	23.57 ± 3.76	32 ± 11
BGO	397.34 ± 1.70	312 ± 11	84.44 ± 7.42	100 ± 11
CsI	943.5 ± 10	720 ± 11	204.5 ± 14.2	204 ± 11

5.2 Background Noise

It can be seen that in absence of radioactive sources an environmental background noise is still present(see figure (11)).
However, as shown in the first part of the characterization of the SiPM, it is not true that there are no sources of photons, since the measurement can be disturbed by the light entering the mini spectrometer.

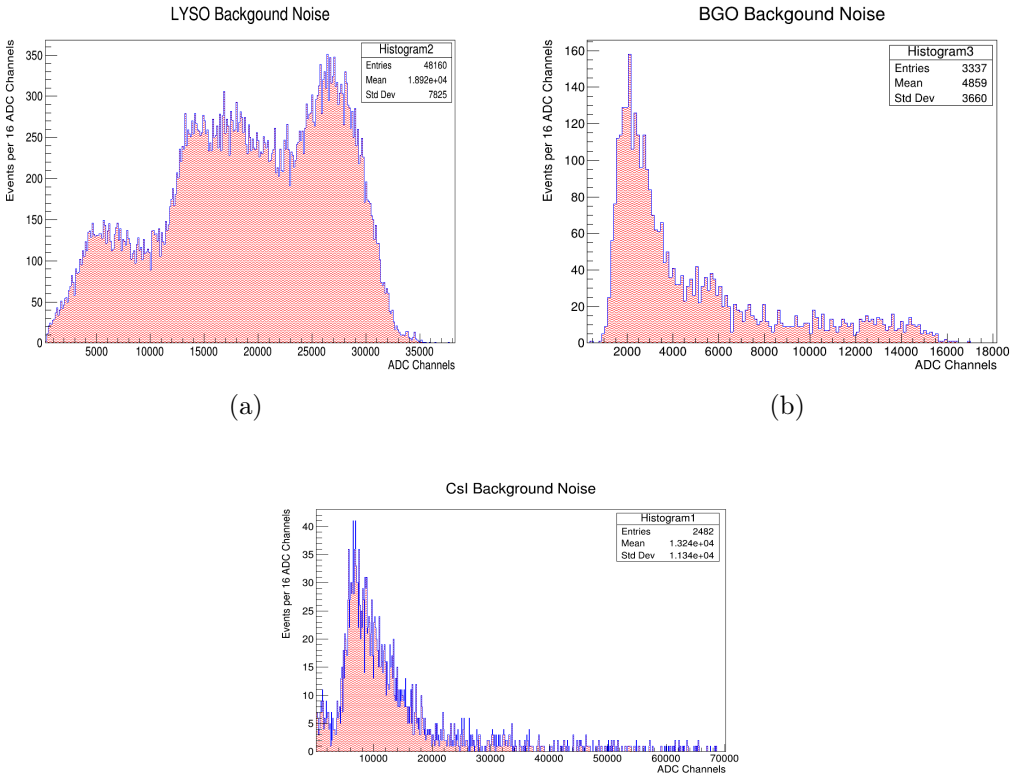

(a) (b)

Figure 11: *Background noise crystals*

5.3 ^{22}Na Spectrum

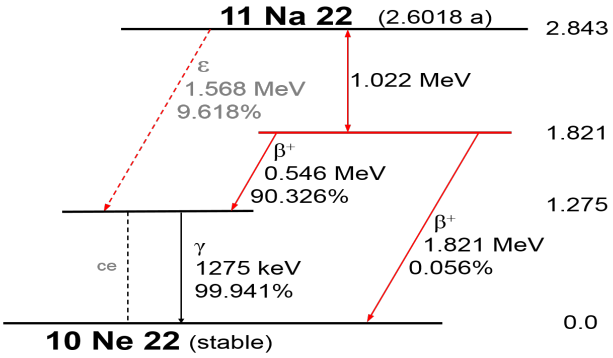

Figure 12: *Decay Scheme of ^{22}Na Spectrum*

Firstly, ^{22}Na (figure12) decays β^+ on an excited state of ^{22}Ne emitting a positron, with an high probability (BR = 90%). Then, it emits a γ (1275 KeV) to reach the ground state. There are very little chances that it decays directly to the ground state (0.06%).
The emitted positron annihilates with an electron of the surrounding matter and leads to a characteristic annihilation radiation at 511 keV, as can be seen in the first peak in figure(13). Because of the conservation of four-momentum, two γ are produced. These photons are emitted in opposite directions.
Peaks are preceded by the Compton edge. The ^{22}Na spectrum obtained with the three scintillators is shown below.

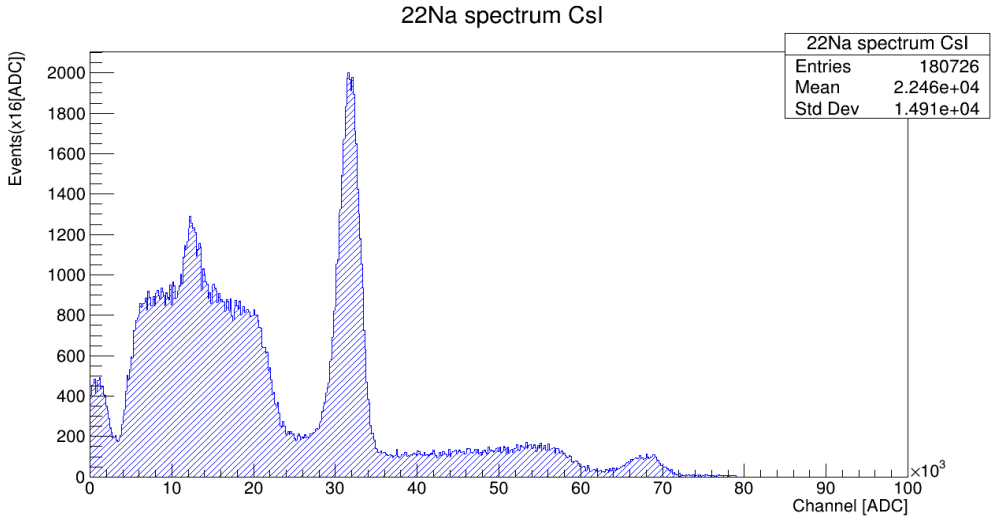

Figure 13: *^{22}Na spectrum with a CsI scintillator.*

5.4 ^{57}Co Spectrum

The decay of ^{57}Co is a β electron capture one.
With an high probability (BR = 99.8 %, figure 14) it decays emitting either a γ of

122 Kev followed by a γ of 14 Kev or just one photon of 136 Kev.

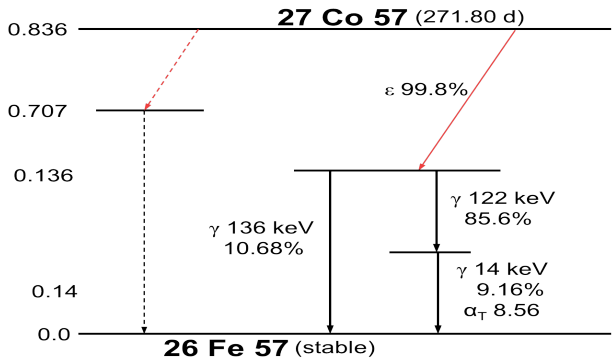

Figure 14: *Decay Scheme of ^{57}Co*

In the spectra below (figure(15)) it is not possible to distinguish the peaks at 122 and 136 Kev, because the difference of energy is too small to be detected.
The peak is preceded by the Compton edge.
The ^{57}Co spectrum obtained with the three scintillators is shown below.

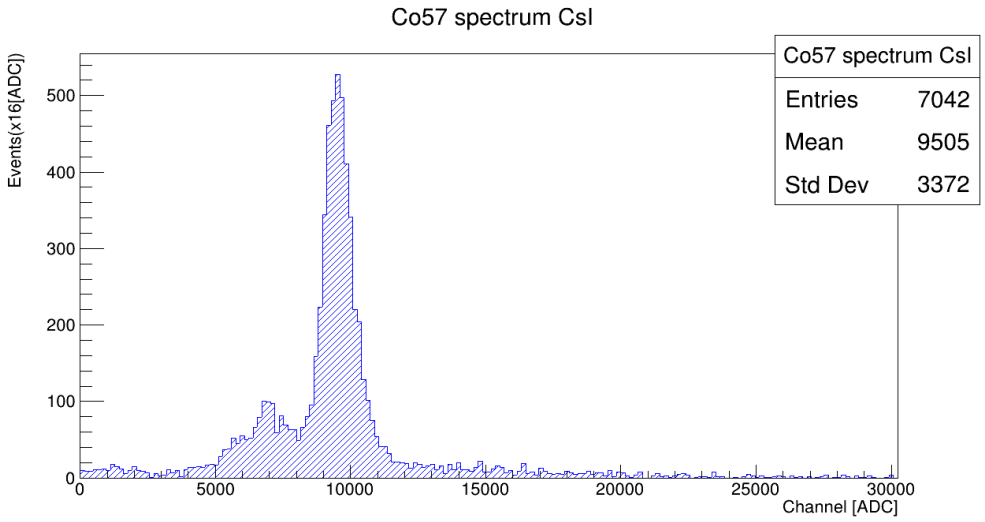

Figure 15: *^{57}Co spectrum with a CsI scintillator.*

5.5 Light Yield

The Light Yield is defined as the number of photons emitted from the scintillator per MeV of absorbed energy. Since it was not possible to determine the precise number of photons absorbed by each pixel of the SiPM, only a ratio of the relative light yield of a scintillator with respect to another could be evaluated. The 511 KeV peak of the ^{22}Na has been fitted with a normal distribution, and the μ (peak position) of the distribution has been chosen for the evaluation of the LY.
The results are shown below.

- 511keV Peak:

$$\frac{LY_{LYSO}}{LY_{CsI}} = 0.6775 \pm 0.0002(tabulated : 0.52) \tag{3}$$

$$\frac{LY_{LYSO}}{LY_{BGO}} = 3.548 \pm 0.001(tabulated : 3.29) \tag{4}$$

$$\frac{LY_{BGO}}{LY_{CsI}} = 0.1909 \pm 0.0001(tabulated : 0.16) \tag{5}$$

Only the 511 KeV peak is clearly distinguishable: the chosen configuration did not allow to see the other 1274KeV peak in every scintillator (CsI is the exception).
For the ^{57}Co the same process has been followed. The 122KeV and the 136KeV peak could not be resolved, therefore the spectrum has been fitted with the same Gaussian. The results are the following:

$$\frac{LY_{LYSO}}{LY_{CsI}} = 0.586 \pm 0.001(tabulated : 0.52) \tag{6}$$

$$\frac{LY_{LYSO}}{LY_{BGO}} = 3.65 \pm 0.01(tabulated : 3.29) \tag{7}$$

$$\frac{LY_{BGO}}{LY_{CsI}} = 0.1602 \pm 0.0006(tabulated : 0.16) \tag{8}$$

5.6 Energy Resolution

Energy resolution is the parameter of a scintillator which expresses its ability to resolve a given peak in relation to its energy. It is expressed as:

$$\epsilon = \frac{FWHM_{peak}}{\mu_{peak}} \tag{9}$$

Where $\text{FWHM}_{\text{peak}}$ is the full width at half maximum of each peak, which is equal to $2\sqrt{2log2} \times \sigma_{peak}$.

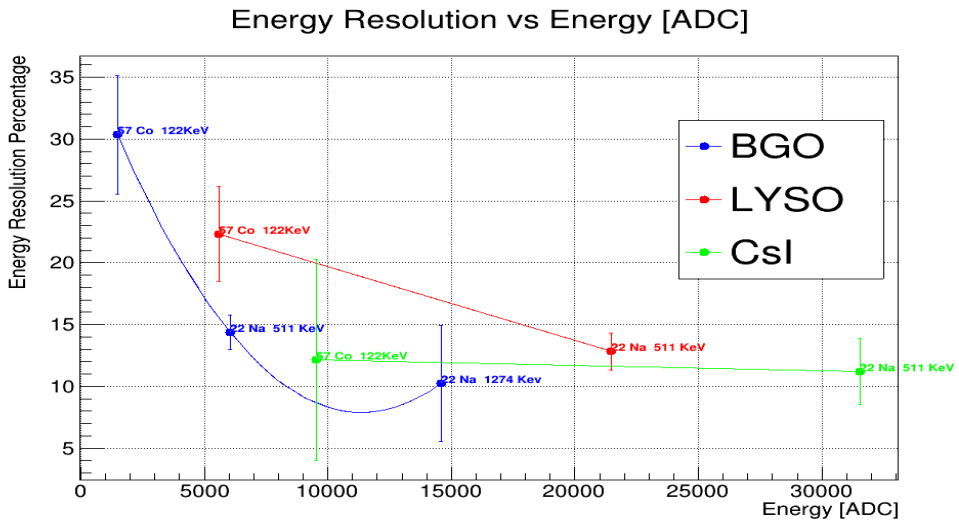

Figure 16: *Energy Resolution*

Figure 16 shows the inverse proportionality between the energy resolution and the energy of a peak, although the functional dependence is not really evident, since the SiPM configuration was not ideal: the 14 KeV peak of the ^{57}Co required a higher light yield to be seen and the 1275 KeV peak of the ^{22}Na was cut off due to a saturation problem.
As expected, the figure shows that for a chosen peak crystals with a better light yield have a worse energy resolution.

5.7 Barycenter of Absorption Crystals

In each crystal there is a "barycenter" of absorption where radiation is absorbed in average. It is possible to give an estimation of this quantity by taking different spectra of ^{22}Na at different distances of the source from the crystal.
The idea is that the flux of photons (height of the photo-peak) decreases with distance as r^2 (figure 17). Therefore, the data are fitted with:

$$f(x) = \frac{A}{(x+D)^2} \tag{10}$$

Where D is the length at which photons are absorbed from the top of the crystal.

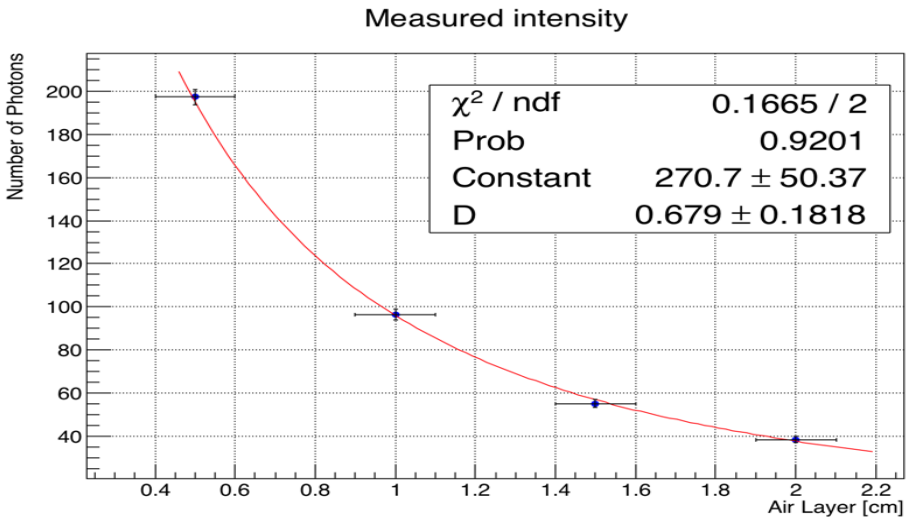

Figure 17: *Barycenter of absorption*

5.8 Absorption

When radiation travels through materials, it loses intensity according to the law:

$$I = I_0 \times e^{-\mu x} \tag{11}$$

The aim of this section is to give an estimation of the value of μ for three different materials (air, plastic and metal) by fitting data with the following equation:

$$y = \log I_0 - |\mu| \times x \tag{12}$$

Where, x is the distance travelled in the material and y is the natural logarithm of the intensity (number of counts of the peak). This is based on the assumption that the intensity of the absorbed radiation is proportional to the number of counts. Since μ depends on the energy, its value for the same material decreases as energy increases(figure (18)). For metal and plastic data have been taken with ^{22}Na.

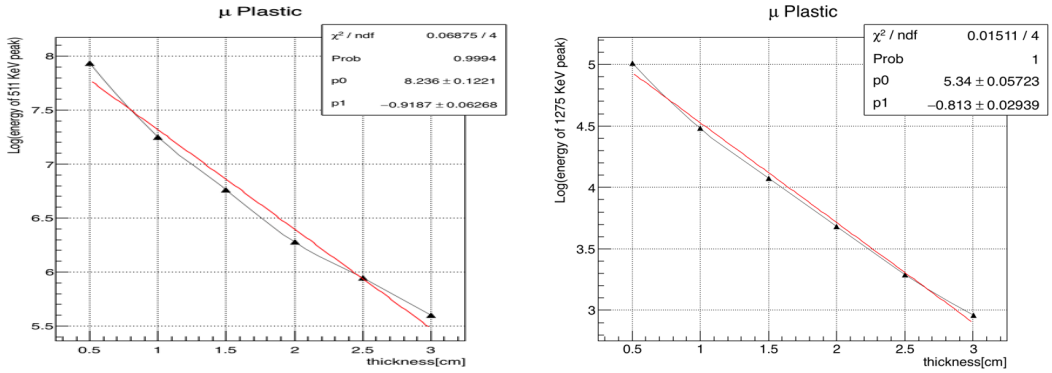

(a) (b)

Figure 18: *Left: air coefficient of absorption for the peak at 511 KeV. Right: air coefficient of absorption for the peak at 1275 KeV. μ decreases when the energy increases.*

Each time an half cm of material was added between the source and the crystal. It is important to outline that for these two measurements (metal and plastic), the distance between the source and the crystal has never been changed. Results:

Material	μ **(511KeV) [cm^{-1}]**	μ **(1275KeV) [cm^{-1}]**
Metal	1.31 ± 0.06	1.29 ± 0.05
Plastic	0.92 ± 0.06	0.83 ± 0.03

Table 2: *Absorption Coefficienct*

As it is possible to see, μ grows increasing the density and the Z of the material(table 2).

5.8.1 The case of Air

For the special case of Air it has not been possible to keep a constant distance between the source and the Crystal. Therefore, it has been necessary to normalize data with respect to the solid angle under which the SiPM sees the source. The surface element (ds) between the radioactive source and the SiPM has been considered a constant.

$$d\Omega = \frac{ds}{r^2} \propto \frac{1}{r^2} \tag{13}$$

So in this case:

$$y = ln(I \times r^2) = lnI + 2lnr \tag{14}$$

Where r is the solid angle radius, which is the distance between source and the point where photons are absorbed. Indeed:

$$r^2 = (d + barycenter)^2 \tag{15}$$

In fact, as it was verified in section (5.8), photons are not absorbed at the top of the crystal, but at a length that has been called barycenter of the crystal.

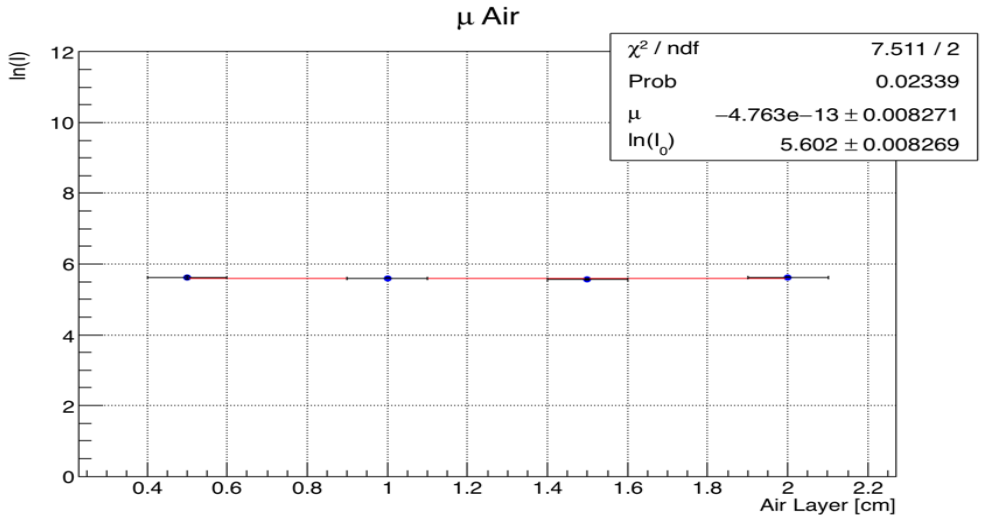

Figure 19: *μ Air*

The absorption coefficient of air is 0 ± 0.008 cm^{-1}, as shown in figure(19).

5.9 Cosmic Rays

Cosmic rays are high energy particles and atomic nuclei which hit the atmosphere at high velocity with different angles. As a consequence of the collision other beams of particles are generated.
It is possible to measure the spectrum of the incident radiation with an apposite detector made of a plastic scintillator read out with a SiPM, as shown in figure (20).

Figure 20: *Plastic Scintillator read out with a SiPM*

Cosmic rays are mostly composed of γ radiation and muons (μ) which are MIP (minimum ionizing particle with an energy of 4 Gev and a flux of 1 particle/cm^2). The resulting spectrum is not a perfect peak centered in the energy of the incident muons because they arrive with different angles (figure(21)).

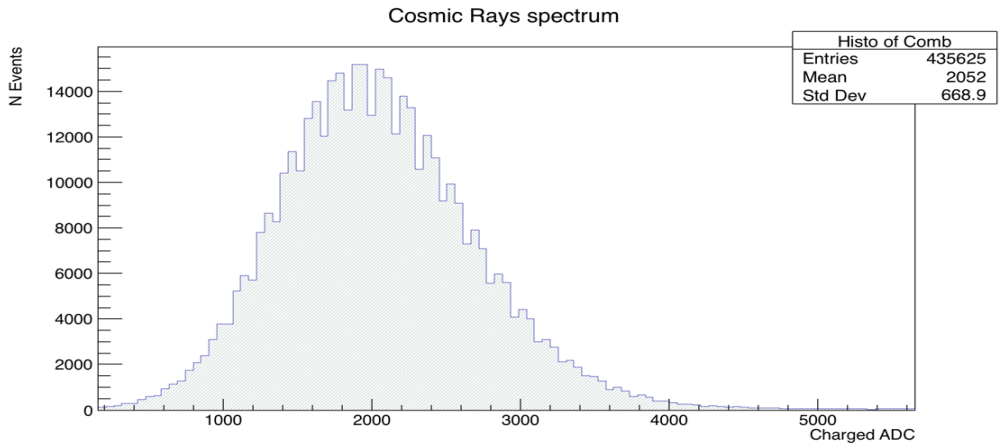

(a)

Figure 21: *Cosmic rays spectrum*

5.10 β Spectroscopy

With a plastic scintillator it is possible to reveal the spectrum of a β radioactive source (^{90}Sr). The decay of ^{90}Sr is a β^-:

$$^{90}Sr \rightarrow ^{90}Y + e^- + \bar{\nu}_e \rightarrow ^{90}Zr + e^- + \bar{\nu}_e \tag{16}$$

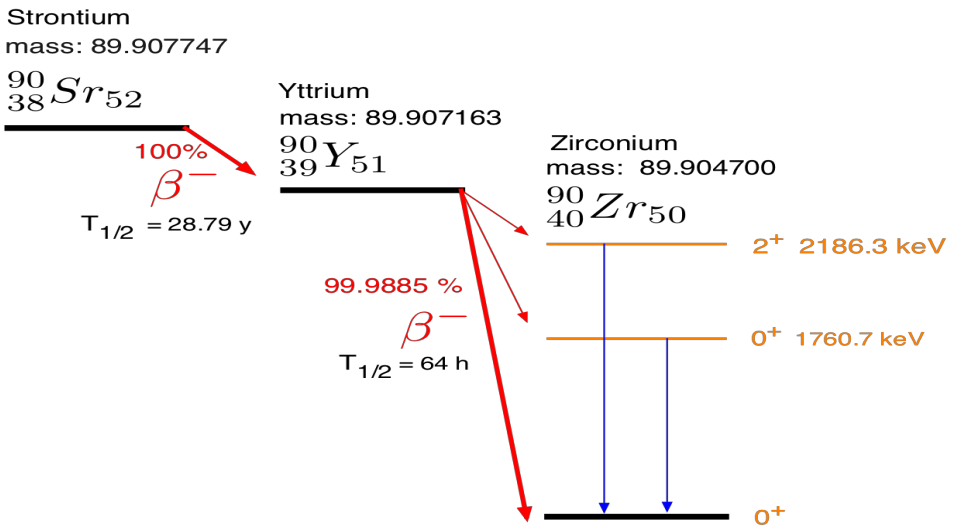

Figure 22: ^{90}Sr β *decay*

The spectrum is a purely beta one, in fact, γ radiation is too energetic to be trapped inside the detector.

A plastic scintillator has a smaller density than the inorganic one, so that, radiation coming from the β decay will not be stopped.

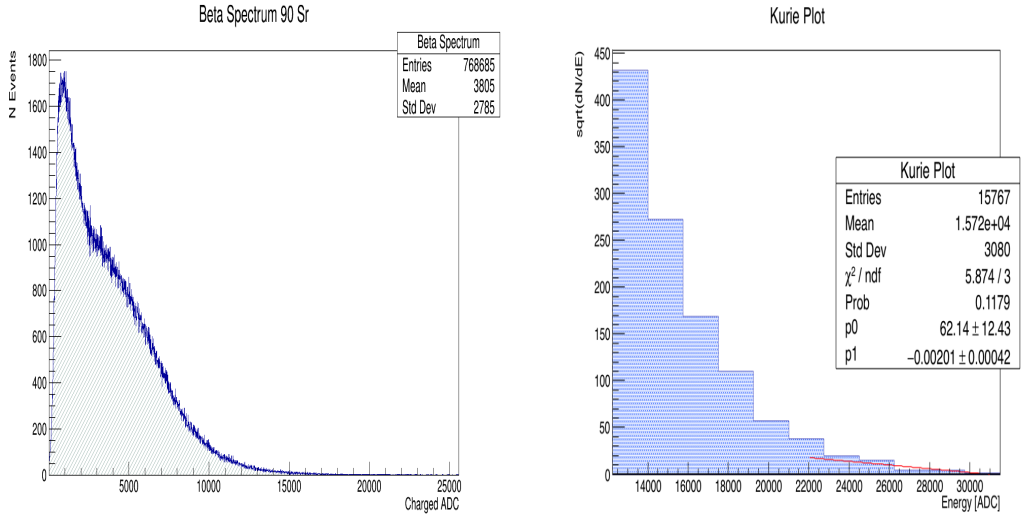

(a) Beta Spectrum (b) Kurie Plot

Figure 23: *β spectrum with plastic scintillator*

The β spectrum is continuum, all particles energies are possible from zero to a maximum called the endpoint energy. The endpoint energy in β decay corresponds to the mass difference between the parent and daughter nuclides.
The endpoint can be estimated either by fitting the β spectrum with an exponential decreasing function or by fitting its Kurie Plot.
In fact, the Kurie plot is a way to linearize the spectrum, in order to estimate at best the maximum energy of the decay. As it can bee seen in figure 23 (b) the kurie plot has not a perfect linear shape because of the resolution of the detector. The y-axis values should be:

$$y = \sqrt{\frac{\frac{dN}{dE}}{F(Z,E) \times S(E)}} \tag{17}$$

Where F(Z,E) and S(E) are corrections to the formula. In Figure 23 (b), these correction have not been taken in account.
The endpoint of the β spectrum changes with the position of the radioactive source in the detector. The tile is a 46mm x 46mm square: as shown in figure(20) the endpoint energy increases with light yield, reaching its maximum value in the centre of the tile, expected.

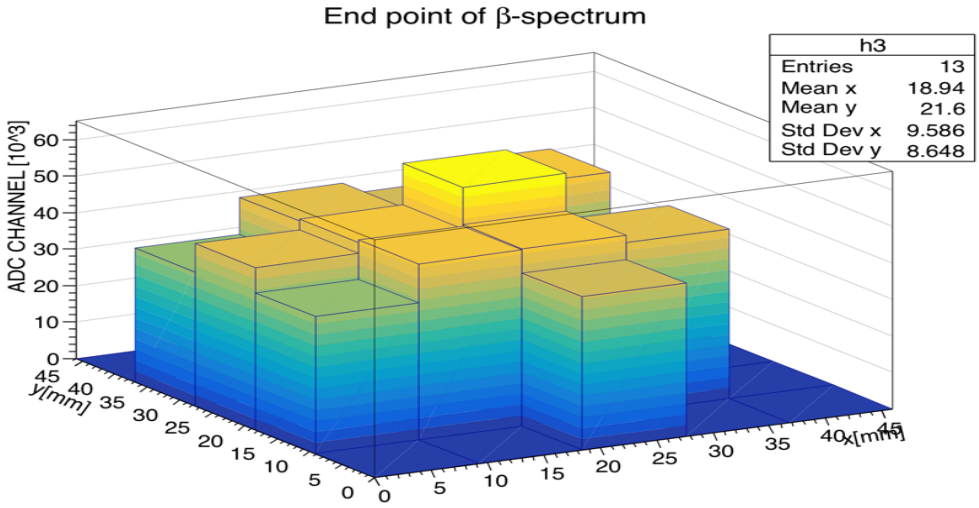

Figure 24: *Endpoint in different points of the tile. Each end point has been computed by fitting each spectra with a decreasing exponential*

6 Conclusion and Comments

- Characterization:
  Dark counts and crosstalk have been characterized for two different SiPM. However, this information resulted negligible for the measurement of the spectroscopy and the LED emitter. The reason is that dark counts are overcame by the counts coming from the light emitter and the radioactive sources.
  In fact, it is possible to see that by decreasing the frequency of the emitting photons the rate of dark count become more significant.
  In the case of the LED emitter(section (4)) the peaks are distributed as a Poisson function(figure 8). If the frequency of hitting photons is increased, the Poisson distribution tends towards a Normal distribution, figure(25).

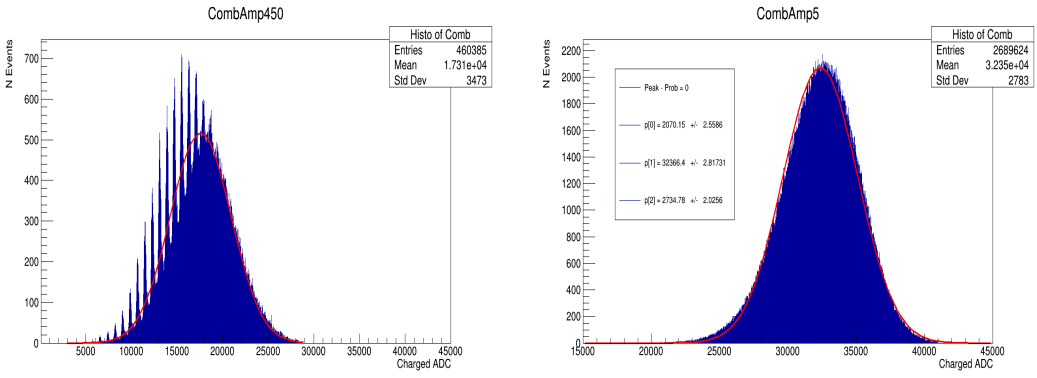

(a) (b)

Figure 25: *Poisson tends to a Normal distribution*

- Crystal Characterization:

Crystals have been characterized in order to find the more suitable for the estimations of the coefficient of absorption of the three materials and for the γ spectroscopy, e.g., CsI has been chosen for the absorption of the radiation by materials since with this is one, the second peak was clearly visible (even though it has the worst energy resolution) of the ^{22}Na avoiding a saturation, as in the case of LYSO. Moreover it has a higher light yield than the other two.
It has been necessary to use grease (*as a matter of fact, too much grease*) in order to optimize the optical coupling of SiPM and the scintillator. In fact, grease has a refracting index similar to that of the photomultiplier: this avoids the entrapment of photons in the crystal.

- β spectroscopy
  For the β spectroscopy a plastic scintillator, capable of holding inside the β radiation, has been utilized.

References

[1] SensL, Introduction to SiPM, Technical Note
[2] CAEN, SP5600AN Guide
[3] CAEN, Educational Catalog